LAWRENCE
LIVERMORE
NATIONAL
LABORATORY

LLNL-CONF-656252

# Double Shock Experiments and Reactive Flow Modeling of High Pressure LX-17 Detonation Reaction Product States

K. S. Vandersall, F. Garcia, L. E. Fried, C. M. Tarver

June 30, 2014

15th International Detonation Symposium
San Francisco, CA, United States
July 13, 2014 through July 18, 2014

## Disclaimer

# Double Shock Experiments and Reactive Flow Modeling of High Pressure LX-17 Detonation Reaction Product States

Kevin S. Vandersall, Frank Garcia, Laurence E. Fried, and Craig M. Tarver

Energetic Materials Center
Lawrence Livermore National Laboratory, Livermore, CA 945550

**Abstract.** Experimental data from measurements of the reaction product states of an energetic material are desired to fully characterize its performance. In a case like LX-17 (92.5% TATB and 7.5% Kel-F by weight), where chemical kinetics cause the evolution of partially reacted states, this information becomes even more vital. Experiments were performed to measure reacted states of LX-17 products using a double shock method involving the use of two flyer materials with known properties mounted on the projectile. This technique sends an initial shock through the material with a pressure near to or above the Chapman-Jouguet (CJ) state, followed by a second shock at a higher magnitude into the reaction products. By measuring the parameters of the first and second shock waves, information on the doubly shocked product states can be obtained. The LX-17 detonation reaction zone profiles plus the arrival times and amplitudes of reflected shocks in LX-17 detonation reaction products were measured using Photonic Doppler Velocimetry (PDV) probes and an aluminum foil coated LiF window. The discussion of this work includes the experimental parameters, velocimetry profiles, data interpretation, reactive CHEETAH and Ignition and Growth modeling, as well as possible future experiments.

## Introduction

The insensitive high explosive (IHE) LX-17 (92.5% TATB, 7.5% Kel-F by weight) has slower reaction kinetics than conventional high explosives, which create a 3 mm detonation reaction zone length [1] and shock front curvature. A double shock technique was chosen to provide a method for measuring the doubly shocked reacted state and any kinetic effects at the rear sample/window interface using Photonic Doppler velocimetry (PDV). The first shock detonates the LX-17, and the second shock then travels through the reacted state. If the reaction in the initial shock is fast and complete, and the difference between the first and second shock pressure is small, then the measured second shock (or re-shock) velocity should be equal to the isentropic (sound) wave speed in the material [2]. If the reaction is incomplete, interpretation is necessary to correlate the second shock wave speed to the true isentropic wave speed. If the difference between the first and second shock pressure is larger (i.e. when the change in the sound speed with second shock pressure is not negligible), then the second shock achieves a colder state at a given pressure than obtained along the first shock Hugoniot at that same pressure. The study of the second shock therefore allows the separation of thermal and compressive terms in the equation of state. Previous research on reflected or overdriven experiments has been performed by a number of

researchers [3-9]. The work here builds on a prior set of experiments performed using reflected shocks with manganin piezoresistive gauges to measure the initial and reflected shocks [10]. This paper discusses: the experimental setup; PDV measured velocities; comparisons to reactive flow modeling; and future work. The overall goal of this work is to measure the reacted equation of state, observe any kinetic time dependent effects in the second shock, and compare to reactive flow models for validation.

**Experimental Procedure**

Experiments were performed using the two-stage gun at Lawrence Livermore National Laboratory (LLNL). Figure 1 contains a schematic of the experiment showing the polycarbonate sabot projectile with a 2 mm thick 304 stainless steel front flyer plate backed with 3 mm of tantalum. The target included a 1.5 mm thick 304 stainless steel buffer plate in contact with LX-17 (TATB based high explosive) that ranged from 3 to 8 mm thick and is backed by 10 mm of LiF as a window for the Photonic Doppler Velocimetry (PDV) probes [11]. A thin 12.7 μm foil of aluminum was placed between the LX-17 layer and the LiF window as a diffuse reflector material. The LX-17 is held in place by a 3 mm thick by 11 mm long retainer ring. 2-d simulations of the experiment included the retainer ring. The retainer ring, LX-17, and buffer plate was held in place by an aluminium fixture. Hydrodynamic simulations showed that the fixture had a negligible effect on the experimental signal. A set of 6 time of arrival shorting pins was used to measure the impact arrival and subsequent tilt. The impact velocity was chosen to result in pressures slightly below, at, or above the CJ pressure for the LX-17 sample. The LX-17 is driven at detonation-like conditions by a supported shock that propagates through the reacting sample. The velocity was recorded using measurements on the x-ray film as well as a series of laser photodiode velocity traps. An array of four PDV probes were used at the back of the target for observing the shock arrival times and interface particle velocity magnitudes. In this paper only the center probe data is reported. Some of the 2-D effects will be discussed by comparison to simulations.

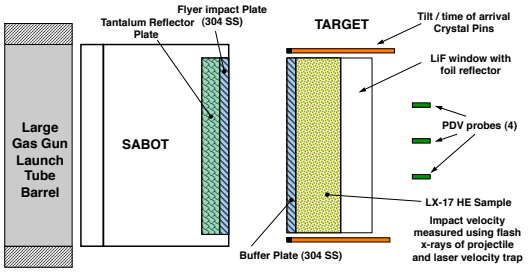


Figure 1. Schematic of the double shock experiments performed using a 2-part flyer impacting a buffer plate, an LX-17 sample backed by a LiF window. A Teflon ring (not shown) surrounds the sample and had holes for the pin were inserted through.

**Reactive Flow Models**

The Ignition and Growth reactive flow model [12] uses two Jones-Wilkins-Lee (JWL) equations of state (EOS), in the temperature dependent form:

$$p = Ae^{-R_1 V} + Be^{-R_2 V} + \omega C_V T / V \quad (1)$$

where p is pressure, V is relative volume, T is temperature, ω is the Gruneisen coefficient, Cv is the average heat capacity, and A, B, $R_1$ and $R_2$ are constants. The reaction rate equation is:

$$dF/dt = \underbrace{I(1-F)^b(\rho/\rho_0 - 1 - a)^x}_{0<F<F_{Ig\max}} + \underbrace{G_1(1-F)^c F^d p^y}_{0<F<F_{G1\max}} + \underbrace{G_2(1-F)^e F^g p^z}_{F_{G2\min}<F<1} \quad (2)$$

where F is fraction reacted, t is time in μs, ρ is current density, $\rho_o$ is initial density, p is pressure in Mbars, and I, $G_1$, $G_2$, a, b, c, d, e, g, x, y, and z are constants. Vandersall et al. [13] listed the detonation modeling parameters. Gustavsen et al. [14] showed the existing data on overdriven states of LX-17 and PBX 9502 (95% TATB/5% KelF) [5,6,13,15]. Figure 2 shows this experimental data and the calculated JWL states. The JWL EOS is accurate for shock velocities exceeding 9 km/s and shock pressures approaching 70 GPa.

Table 1. Comparison of Ignition and Growth and ALE3D/CHEETAH detonation model framework.

| Detail | Traditional reactive flow (Ignition & Growth) | ALE3D / Cheetah |
|---|---|---|
| Species set | Reactant, product | > 30 chemical compounds |
| Reaction rate | 3 step reaction | Multiple reaction |
| Rate forms | Pressure and compression dependent | Pressure or temperature dependent |
| Gas EOS | JWL | Exp-6 + dipole fluid model |
| Solid EOS | JWL | Extended Murnaghan |
| Phases | 2 | > 3 |

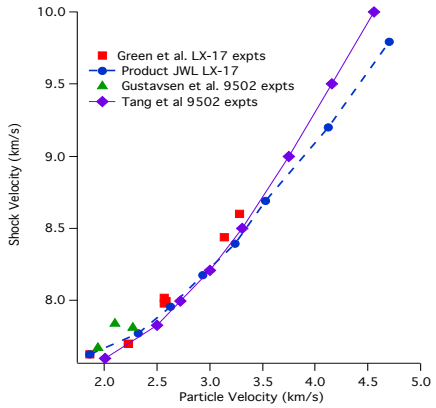


Figure 2. Shock velocity - particle velocity data for LX-17 and PBX 9502 overdriven detonations.

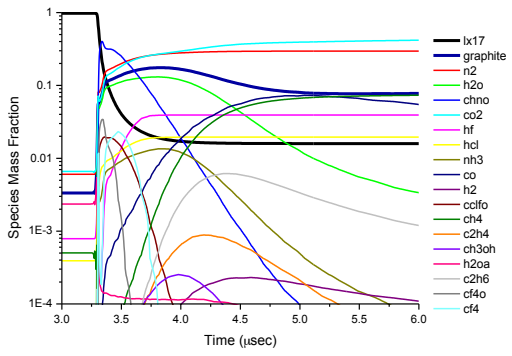


Figure 3. Plot of species mass fractions as a function of time for the CHEETAH detonation model.

CHEETAH detonation models are based on a multiscale approach to HE detonation modelling and is linked into the ALE3D code [16]. The CHEETAH detonation model includes more EOS features than a traditional model. A comparison of the model basis is shown in Table 1. Figure 3 shows an output of the species set mass fraction as a function of time. The current Cheetah detonation models are typically applied to steady detonation. This version does not incorporate "fast kinetics" to simulate "re-equilibration" of reaction products, although this will be added in the near future.

**Results and Discussion**

The experimental details for the series of double shock experiments are shown in Table 2 including the experiment number, date fired, impact velocity, and component dimensions. In the experiments, the thickness of the LX-17 samples was varied to provide some comparison information about the evolution of the wave as a function of distance travelled. The flyer velocities are sufficiently high to cause rapid initiation of detonation in LX-17 by the shock waves from the steel impact. The impact of the tantalum part of the flyer then creates a second shock in the LX-17 products. The impact of the doubly shocked reaction products on the higher impedance aluminum coated LiF crystal causes a reflected shock to propagate back into the LX-17 reaction products. Depending on the thickness of the LX-17 layer, this shock reflection can occur before the arrival of the shock produced by the tantalum layer, resulting in a more complex interface particle velocity flow. Although two shocks are driven into the LX-17, and two shocks are measured in most experiments, it is important to realize that there are multiple shock wave interactions occurring in the experiment. The hydrodynamic reactive flow models must account for all these interactions plus the reaction rates and EOS states of LX-17 products shocked to various pressures.

Figures 4 and 5 display the center PDV probe signals for the first four experiments outlined in Table 2. Although only the center probes are shown, the center probes were compared to three redundant probes on an outer perimeter. These

probes showed some variation, possibility due to projectile tilt and in the thickest sample the rarefaction release waves from the edges. The experimental results are compared to 2D Ignition and Growth and Cheetah detonation modelling in order to gain an understanding of kinetic effects.

As seen in Figs. 4 and 5, the shape of the second shock wave shows a more "rounded" front for all experiments that most probably indicates some product reaction kinetic effects in the doubly shocked high pressure, high temperature LX-17 products. Such a "re-equilibration" process in detonation reaction products has never previously been measured. If this phenomenon does occur, it is unrealistic to expect the current reactive flow models, which do not contain a chemical kinetic "re-equilibration" model, to yield perfect agreement with the experimental data.

The basic features in the experiments are reproduced in the comparisons of the model to the data. In experiments 4109 and 4110 outlined in Fig. 4, the initial shocks and LX-17 reaction zone profiles are seen in both experiment and calculations. Simulations are shown aligned to the experimental first arrival time. The calculated second shock arrival timings are close to those measured experimentally. The rounding of second shock is observed in the experimental data, but not in the model results. Both the Ignition and Growth and Cheetah second shock interface particle velocities are higher than experimentally measured. The Cheetah results are closer to the experimental records. Recall that the double shock experiment will be colder than a single shock experiment at the same pressure. Since the Ignition and Growth and Cheetah models match overdriven single shock experiments, the overprediction of the second shock velocities most likely indicates that the EOS models used in the models have thermal effects that are too small.

For the slightly higher velocity experiments in Fig. 5, experiment 4111 shows the initial shock and decay in the experiment with rounding of second shock. Experiment 4112 shows a similar behavior, although, due to the thin 3 mm thick LX-17 layer, a third shock wave is observed at a later time. The comparison with the modeling results again provides an overall general agreement but not an exact match of profile. Both models again predict higher velocities than measured, and the Cheetah results are closer to the measurements.

Table 2. Experimental details for the double shock experiments including component dimensions.

| Expt, Date | Velocity (km/s) | Rear Flyer | Front Flyer | Buffer Plate | LX-17 | Reflector | LiF |
|---|---|---|---|---|---|---|---|
| 4109, 4/18/12 | 3.511 km/s | Ta, 3.022 mm | 304 SS, 2.019 mm | 304 SS, 1.508 mm | 19 mm Ø by 8.013 mm | 12.7 µm Al | 19 mm Ø by 10.016 mm |
| 4110, 4/20/12 | 3.518 km/s | Ta, 3.018 mm | 304 SS, 2.020 mm | 304 SS, 1.509 mm | 19 mm Ø by 5.995 mm | 12.7 µm Al | 19 mm Ø by 10.078 mm |
| 4111, 4/24/12 | 3.916 km/s | Ta, 3.016 mm | 304 SS, 2.018 mm | 304 SS, 1.495 mm | 19 mm Ø by 5.015 mm | 12.7 µm Al | 19 mm Ø by 10.031 mm |
| 4112, 4/26/12 | 3.737 km/s | Ta, 3.020 mm | 304 SS, 2.023 mm | 304 SS, 1.496 mm | 19 mm Ø by 3.014 mm | 12.7 µm Al | 19 mm Ø by 10.028 mm |
| 4178, 8/7/13 | 2.49 km/s | Ta, 3.019 mm | 304 SS, 2.022 mm | 304 SS, 1.507 mm | 19 mm Ø by 5.013 mm | 12.7 µm Al | 19 mm Ø by 10.044 mm |
| 4179, 8/9/13 | 4.90 km/s | Ta, 3.019 mm | 304 SS, 2.023 mm | 304 SS, 1.516 mm | 19 mm Ø by 5.017 mm | 12.7 µm Al | 19 mm Ø by 10.036 mm |
| 4180, 8/13/13 | 3.35 km/s | Ta, 3.020 mm | 304 SS, 2.020 mm | 304 SS, 1.517 mm | 19 mm Ø by 6.021 mm | 12.7 µm Al | 19 mm Ø by 10.083 mm |
| 4181, 8/15/13 | 4.67 km/s | Ta, 3.020 mm | 304 SS, 2.022 mm | 304 SS, 1.520 mm | 19 mm Ø by 6.002 mm | 12.7 µm Al | 19 mm Ø by 10.030 mm |

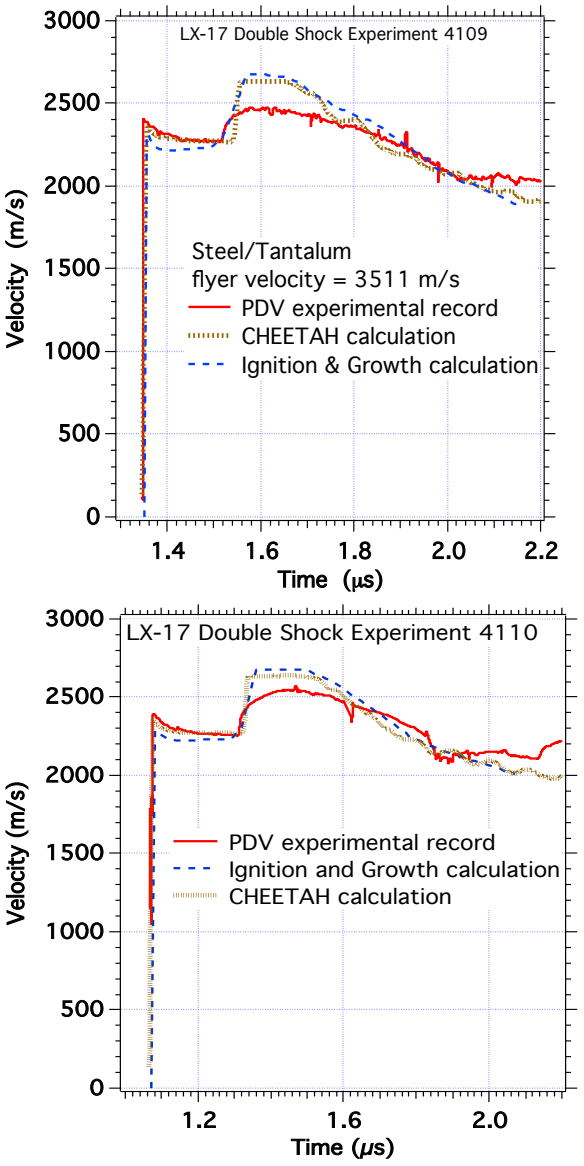


Figure 4. Comparison of experimental and modelling results for experiment (top) 4109 with a 3.51 km/s impact velocity and 8 mm thick LX-17 sample and experiment (bottom) 4110 with a 3.52 km/s impact velocity and 6 mm thick LX-17 sample.

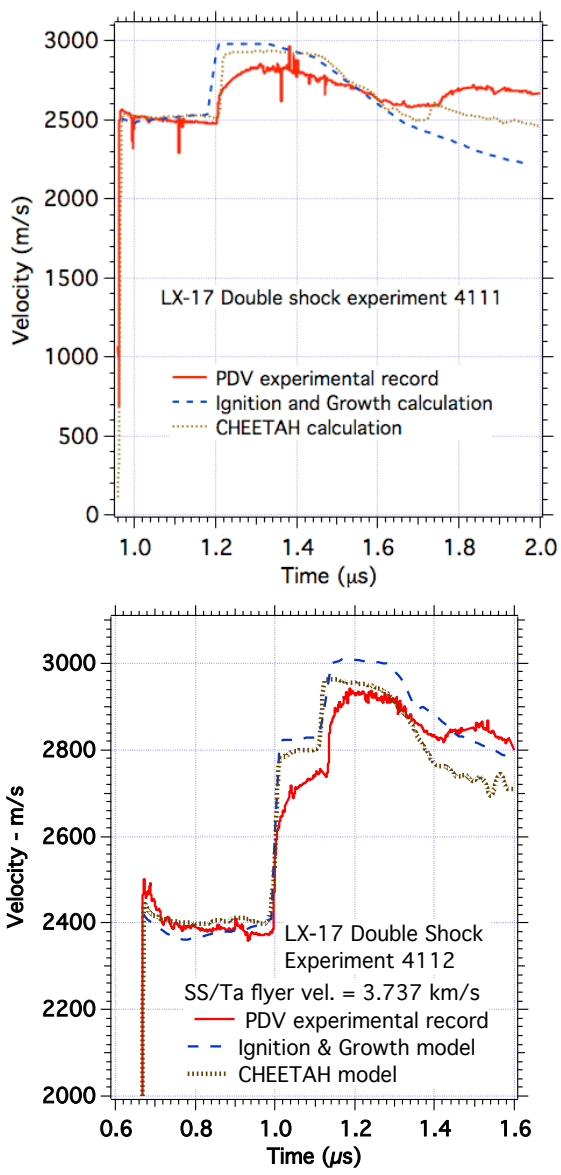


Figure 5. Comparison of experimental and modelling results for experiment (top) 4111 with a 3.92 km/s impact velocity and 6 mm thick LX-17 sample and experiment (bottom) 4112 with a 3.73 km/s impact velocity and 3 mm thick LX-17 sample.

The interface particle velocities measured in four more recent experiments with lower and higher flyer velocities listed in Table 2 are shown in Figs. 6 – 9. The Ignition and Growth and Cheetah comparisons are also shown. The same trends are apparent as those seen in Figs. 4 and 5. The initial shock fronts and reaction zone profiles plus the arrival times of the second shocks from both the Cheetah and Ignition and Growth models agree well with experiment. Both reactive flow models predict higher interface particle velocities than the experimental measurements. Again the Cheetah predictions are closer to experiment than the Ignition and Growth predictions.

The better agreement observed in the second and third shock regimes produced by the Cheetah code compared to those from the Ignition and Growth model is due to the more detailed description of the reaction product EOS at these extreme pressures and temperatures. The JWL product EOS is a six-parameter equation fit to the single shock product Hugoniot data, as shown in Fig. 2. When these products are re-shocked once or twice, the resulting compression states may not be accurate. They could over or under predict the degree of compression in the second shock wave. Since Cheetah is based on a complex potential interaction scheme between the various product species, it potentially has the ability to yield better descriptions of the multiply shocked products.

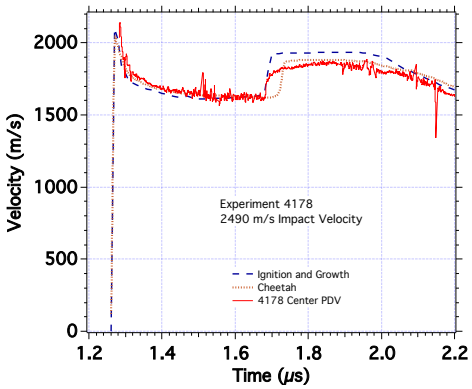


Figure 6. Comparison of experimental and modelling results for experiment 4178 with a 2.49 km/s impact velocity and 5 mm thick LX-17 sample.

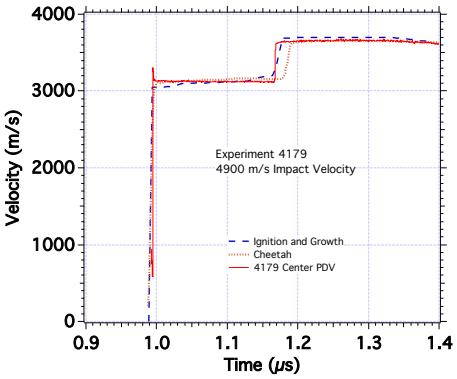


Figure 7. Comparison of experimental and modelling results for experiment 4179 with a 4.90 km/s impact velocity and 5 mm thick LX-17 sample.

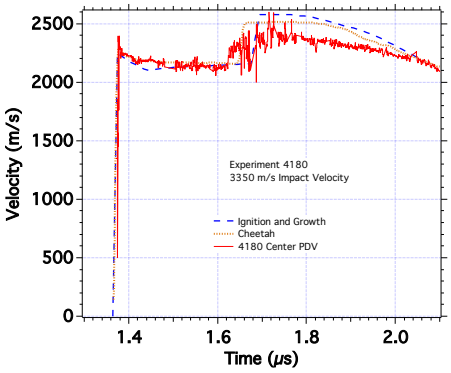


Figure 8. Comparison of experimental and modeling results for experiment 4180 with a 3.35 km/s impact velocity and 6 mm thick LX-17 sample.

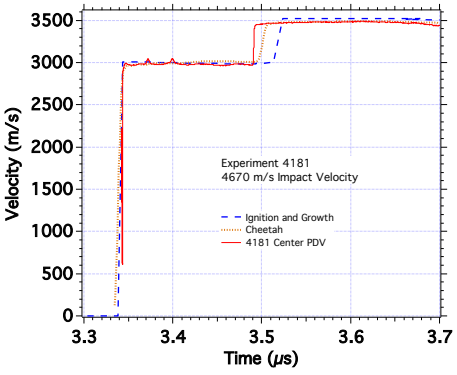


Figure 9. Comparison of experimental and modeling results for experiment 4181 with a 4.67 km/s impact velocity and 6 mm thick LX-17 sample.

The measured interface velocities were converted to pressures as a function of time by impedance matching to the LiF window and are shown in Figs. 10 and 11. The impedance matching procedures rely on the continuity of the pressure and particle velocity across the LiF/ LX-17 interface. The thin reflector material is assumed to make a negligible contribution to the measured particle velocity. A linear Us-Up relation from Marsh [17] was used for the LiF equation of state. The impedance matching analysis ignored the difference in pressure between first and second shock states in the LiF. Calculations with Cheetah using a thermal equation of state for LiF demonstrated that there was less than 0.1 GPa difference in pressure between a first and second shock state in LiF for typical first and second shock pressures of 40 and 50 GPa, respectively. The first shock states are between 30 and 80 GPa, while second shock states are between 35 and 95 GPa. The difference between the first and second shock state is typically 10-20 GPa. The second shocks are sufficiently strong that second shock wave speeds are expected to significantly exceed the sound speed in the first shocked state.

The impedance matching procedure is applicable to one-dimensional flow. As rarefaction waves travel toward the center of the charge, the flow becomes two-dimensional. We have estimated the time of one-dimensional flow by performing hydrodynamic simulations in both planar 1-d and cylindrical 2-d symmetries. In Figure 12, we compare 1-d and 2-d calculations for experiment 4109. In general, 2-d simulations more closely match experiment than the 1-d simulations. We find that 1-d flow is maintained until after the arrival of the second shock. Additional simulations confirmed that this was true for all experiments reported here.

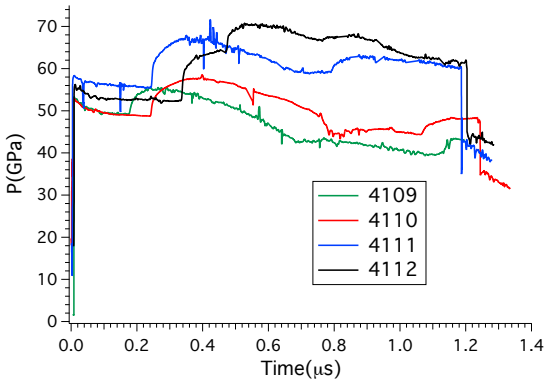


Figure 10. Plot of experimental pressures vs. time found by impedance matching to LiF for experiments 4109 to 4112.

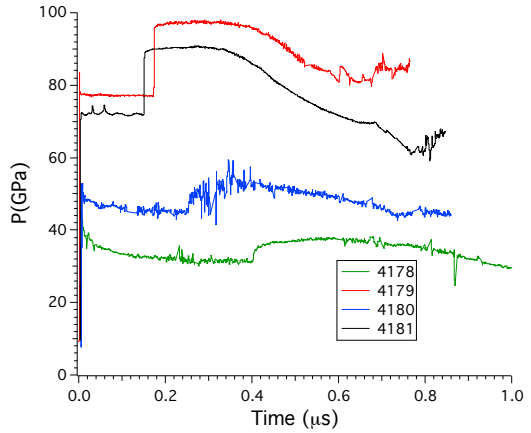


Figure 11. Plot of experimental pressures vs. time found by impedance matching to LiF for experiments 4178 to 4181.

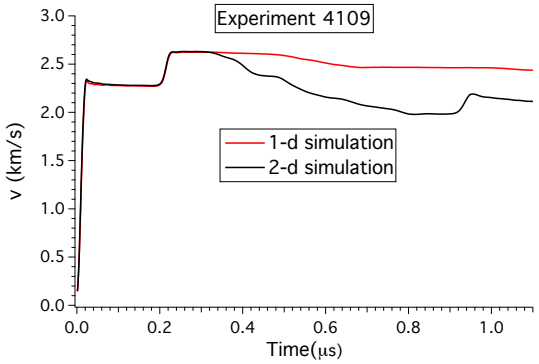


Figure 12: Comparison of one-dimensional and two-dimensional simulations of the double shock experiment.

## Conclusions

A double impactor method was used to measure the reacted equation of state in LX-17. These experiments utilized a PDV technique to measure the double shock at the interface with a LiF window. Comparisons of the experimental data to Ignition and Growth and Cheetah detonation models revealed that the main features matched reasonably well, but some differences still need to be resolved. The experimentally measured "roundings" of the second shock waves are very interesting. These structures are possibly a result of re-equilibration reaction kinetics in the high pressure, high temperature LX-17 reaction products. The Cheetah chemical equilibration code has the capability to determine what chemical species and/or concentrations may be changing in the second shock regime. One possibility is the state of the solid carbon products. At C-J detonation pressure and temperature, TATB forms mainly graphite nanoparticles, but, at higher pressures and temperatures, diamond may be the preferred form of carbon. Carbon nitrides are also possibilities. Re-equilibration of the gaseous products amongst themselves could also occur. Dissociation and/or ionization of certain products are also possible. An analytical EOS form like the JWL equation can be refitted to match the second and third shock states but cannot explain the underlying cause of these experimental results.

Future Cheetah reactive flow modeling is planned to help identify the causes of the differences with the experimental results. Future experiments are in progress using a similar target configuration with the two-stage gun over a wider range of overdriven pressures and different initial LX-17 states.

## Acknowledgements

Special thanks go to Ricky Chau and the gas gun crew of Sam Weaver, Cory McLean, Steve Caldwell, and Bob Nafzinger for their hard work firing the experiments. This work performed under the auspices of the U.S. Department of Energy by Lawrence Livermore National Laboratory under Contract DE-AC52-07NA27344.

## References

1. Tarver, C. W., Kury, J. W., Breithaupt, R. D., "Detonation Waves in Triaminotrinitrobenzene", *J. Appl. Phys.,* Vol. 82, pp. 3771-3782, 1997.

2. Fickett, W. and Davis, W. C., "Detonation," *University of California Press*, Berkeley, CA, 1979.

3. McQueen, R. G., Hopson, J. W., and Fritz, J. N., "Optical Techniques for Determining Rarefaction Wave Velocities at very High Pressures," *Rev. Sci. Instrum*., Vol. 53, pp. 245-250, 1982.

4. Fritz, J. N., "Waves at High-Pressure and Explosive-Products Equation of State," *AIP Conference Proceedings 505*, pp. 239-244, AIP Press, New York, 2000.

5. Fritz, J. N., Hixson, R. S., Shaw, M. S., Morris, C. E., and McQueen, R. G., "Overdriven Detonation and Sound Speed Measurements in PBX 9501 and the "Thermodynamic Chapman-Jouguet Pressure," *J. Appl. Phys*., Vol. 80, pp. 6129-6141, 1996.

6. Green, L., Lee, E., Mitchell, A., and Tarver, C., "The Supracompression of LX-07, LX-17, PBX-9404, and RX-26-AF and the Equations of State of the Detonation Products," *Proceedings of the 8th Detonation Symposium,* pp. 587-595, Albuquerque, NM, July 1985.

7. Green, L. G., Tarver, C. M., and Erskine, D. J., "Reaction Zone Structure in Supracompressed Detonating Explosives," *Proceedings of the 9th Detonation Symposium*, pp. 670-682, Portland, OR, August 1989.

8. Tarver, C. M., Urtiew, P. A., and Tao, W. C., "Effects of Tandem and Colliding Shock Waves on the Initiation of Triaminotrinitrobenzene," *J. Appl. Phys.,* Vol. 78, pp. 3089-3095, 1995.

9. Tarver, C.M. Cook, T. M., Urtiew, P. A., and W.C. Tao, W. C., "Multiple Shock Initiation of LX-17," *Proceedings of the 10th Detonation Symposium*, pp. 696-703, Boston, MA, July 1993.

10. Vandersall, K. S., Forbes, J. W., Tarver, C. M., Urtiew, P. A., and Garcia, F., "Re-Shock Experiments in LX-17 to Investigate Reacted

Equation of State," *AIP Conference Proceedings 620*, AIP Press, New York, pp. 153-156, 2002.

11. Strand, O. T., Goosman, D. R., Martinez, C., Whitworth, T. L., and Kuhlow, W. W., "Compact System for High Speed Velocimetry using Heterodyne Techniques," *Rev. Sci. Instrum*., Vol. 77, 083108, 2006.

12. Tarver, C. M., Hallquist, J. O., and Erikson, L. M., "Modeling Short Pulse Duration Shock Initiation of Solid Explosives," *Proceedings of the 8TH Detonation Symposium*, pp. 951-961, Albuquerque, NM, July1985.

13. Vandersall, K. S., Garcia, F., Tarver, C. M., and Fried, L. E., "Shock Desensitization Experiments and Reactive Flow Modeling on Self -Sustaining LX-17 Detonation Waves," this Symposium.

14. Gustavsen, R. L., Aslam. T. D., Bartram, B. D., and Hollowell, B. C., "Plate Impact Experiments on the TATB Based Explosive PBX 9502 at Pressures near the Chapman-Jouguet State," *Journal of Physics: Conference Series*, IOP Publishing, London, 052015, 2014.

15. Tang, P. K., Anderson, W. W., Fritz, J. N., Hixson, R. S., and Vorthman, J. E., "A Study of the Overdriven Behaviors of PBX 9501 and PBX 9502," *Proceedings of the 11th Detonation Symposium*, pp. 1058-1064, Snowmass, CO, August 1998.

16. Kuo, I. W., Bastea, S., and Fried, L. E., "Reactive Flow Modeling of Liquid Explosives via ALE3D/Cheetah Simulations," *Proceedings of the 14th Detonation Symposium*, pp. 333-337, Coeur d'Alene, ID, April 2010.

17. Marsh, S. P., "LASL Shock Hugoniot Data", University of California Press, Berkeley and Los Angeles, California, 1980.

**Discussion Question**

**Tariq Aslam, Los Alamos National Laboratory**

Were the computational results shifted in time to match the first shock time of the experiments? Was this to account for tilt or multi-dimensional effects?

**Reply by Kevin S. Vandersall**

Yes, the computational results in this work for the center probes were shifted to align at the initial shock arrival time. This was done mainly as a result of the tilt effects observed from experiment to experiment. Doing this appeared reasonable because the main measurement involves the timing and magnitude differences of the first and second shocks. Modeling in 3-D is currently being conducted to characterize the tilt and multi-dimensional effects of the outer PDV probes with comparison to the experiment and these results will be included in a later publication.